ACS OMEGA

http://pubs.acs.org/journal/acsodf

Article

Revisiting Sodium Hexafluoroiridates: Perspective Precursors for Electronic, Quantum, and Related Materials

Alexander I. Gubanov,* Anton I. Smolentsev, Evgeny Filatov, Natalia V. Kuratieva, Andrey M. Danilenko, and Sergey Vasilievich Korenev

Cite This: *ACS Omega* 2021, 6, 27697−27701

Read Online

ACCESS | Metrics & More | Article Recommendations | Supporting Information

ABSTRACT: The following salts have been synthesized and structurally characterized: $Na_2[IrF_6]\cdot 2H_2O$ ($C2/m$, a = 6.6327(4), b = 10.0740(6), c = 5.9283(5) Å, β = 122.3880(10)°) and $Na_3[IrF_6]\cdot 2H_2O$ (R-3, a = 7.5963(3), b = 7.5963(3), c = 9.8056(4) Å) (for the first time) by single-crystal X-ray diffraction; the unit cell parameters of a tetragonal phase ($P4_2/mnm$, a = 5.005(2), c = 10.074(4) Å) of the stable α-$Na_2[IrF_6]$ were determined for the first time; and the unit cell parameters of β-$Na_2[IrF_6]$ ($P321$, a = 9.332(4), c = 5.136(2) Å) and $Na_3[IrF_6]$ ($P2_1/n$, a = 5.567(4), b = 5.778(4), c = 8.017(2) Å, β = 90.41(2)°) were determined using powder X-ray diffraction (PXRD). The data of the thermal stability was obtained by differential thermal analysis (DTA) for all substances. The presence of $Na_3[IrF_6]\cdot H_2O$ monohydrate is predicted. $H_2[IrF_6]$ was prepared in a solution and was demonstrated to behave as a strong dibasic acid.

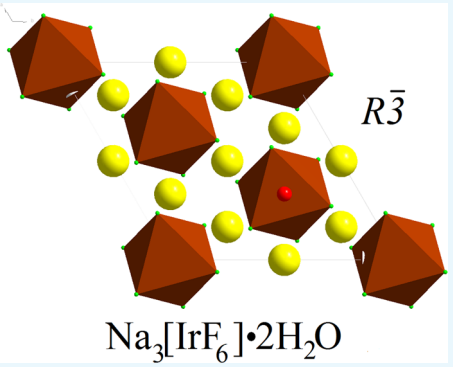

1. INTRODUCTION

Nowadays, paramagnetic complexes of iridium(IV) are considered as promising building blocks for designing electronic and magnetic quantum materials.[1,2] Earlier studies were essentially focused on oxoiridates with the principal structural fragment $\{IrO_6\}^{8-}$, and these compounds have been demonstrated to possess some intriguing physical properties, such as Mott spin−orbit insulators,[3] superconductors,[4−6] Weyl semimetallics,[7−11] spin liquids and ices,[12−15] and ferromagnets with anomalous Hall effect (AHE).[16] With expectations that materials containing $[IrF_6]^{2-}$ fragments also can exhibit specific physical properties,[17] some efforts for the investigation of the electronic structures of $(PPh_4)_2[IrF_6]\cdot 2H_2O$, $Zn(viz)_4[IrF_6]$, $(PPh_4)_2[IrCl_6]$,[18] $A_2[IrF_6]$ (A = Na, K, Rb, Cs), and $Ba[IrF_6]$[19] as well as the crystal structures of $(PPh_4)_2[IrF_6]\cdot 2H_2O$, $Zn(viz)_4[IrF_6]$,[18] Li_2RhF_6, K_2IrF_6,[20] Rb_2IrF_6,[21] Cs_2IrF_6,[22] $Ca[IrF_6]\cdot 2H_2O$, $Sr[IrF_6]\cdot 2H_2O$, and $Ba[IrF_6]$[23] have been undertaken. The most convenient precursor for the synthesis of diverse hexafluoroiridates (IV) involving different cations is the salt $Na_2[IrF_6]$. As a rule, sodium salts of iridates are well soluble in water and therefore are handy starting compounds for ligand substitution reactions[24] as well as cation metathesis.[21−23] Although $Na_2[IrF_6]$ has been known for a long time and its unit cell parameters have been reported ($P321$, a = 9.34 Å, c = 5.14 Å),[25] followed by structural refinement in 2016 ($P321$, a = 9.32858(24) Å, c = 5.13417(19) Å),[18] there are lacunas in the data on the structures of sodium fluoroiridates including the structure of the stable tetragonal phase $Na_2[IrF_6]$. Anhydrous sodium fluoroiridates (III) and (IV), as well as crystal hydrates commonly occurring on the crystallization of aqueous solutions, lack both powder and single-crystal structural data. These findings suggest that the studies on the preparation and structures of sodium fluoroiridates need to be revised.

2. EXPERIMENTAL SECTION

The PXRD experiments were examined on a DRON-RM4 diffractometer (Cu Kα source, graphite monochromator at the diffracted beam, room temperature, 2θ range 5−60°). The experimental data were processed with PowderCell program v.2.4.[26] The data from the powder structural database PDF[27] have been used as standards.

The single crystals were examined on an automated Bruker Nonius X8 APEX diffractometer (MoKα radiation 0.71073 Å, graphite monochromator, CCD detector) at 150(2)K. The reflection intensities were measured by φ scanning of narrow (0.5°) frames. Absorption is taken into account empirically using the SADABS program.[28] Structures were solved by the direct methods of the difference Fourier synthesis and further refined by the full-matrix least-squares method using the SHELXTL package.[29] Atomic thermal parameters for non-

Received: May 26, 2021
Accepted: October 4, 2021
Published: October 14, 2021

https://doi.org/10.1021/acsomega.1c02722
ACS Omega 2021, 6, 27697−27701

hydrogen atoms were refined anisotropically. The positions of hydrogen atoms for water molecules are not located.

A thermal analysis was performed on an "STA 449 F1 Jupiter" in a platinum crucible under a helium atmosphere in the temperature range 25−500 °C.

3. RESULTS AND DISCUSSION

***β*-Na$_2$[IrF$_6$] (I)** was prepared according to the literature method[18] via the treatment of solid $Na_2[IrCl_6]$ with gaseous fluorine under dynamic heating up to 300 °C in a flow reactor. $Na_2[IrCl_6]$ was prepared from commercial "$IrCl_4{\cdot}2H_2O$" in few steps ("The Gulidov Krasnoyarsk Non-Ferrous Metals Plant" Open Joint Stock Company, 51.9% iridium) by dissolution in concentrated hydrochloric acid, followed by the addition of the stoichiometric amount of NaCl and concentration to afford the dry salt. The attempted recrystallization of ***β*-Na$_2$[IrF$_6$] (I)** from aqueous solutions yielded single crystals of **Na$_2$[IrF$_6$]·2H$_2$O (II)** but not those of **(I)**. We expect that they can be prepared by recrystallization from anhydrous HF; however, such an experiment has not been carried out for technical reasons. Then, the powder of **(I)** has been examined with powder X-ray diffraction (Figure 1).

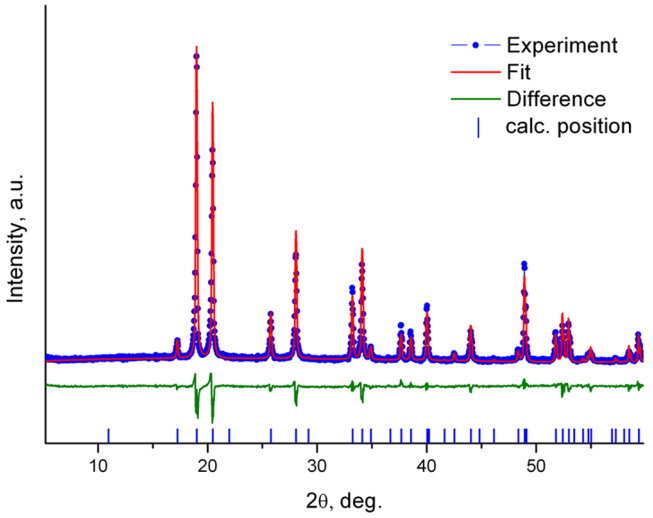

Figure 1. Powder diffraction pattern of ***β*-Na$_2$[IrF$_6$] (I)** and its full-profile refinement.

The powder diffraction pattern of compound ***β*-Na$_2$[IrF$_6$] (I)** was simulated by the full-profile technique using the crystal data of an isostructural compound $Na_2[SiF_6]$[30,31] (Figure 1), as, according to Babel,[31] ***β*-Na$_2$[IrF$_6$]** belongs to the structural type of $Na_2[SiF_6]$ (rhombohedral cell, space group *P*321). The refinement of the unit cell parameters afforded the following values: sp. gr. *P*321, a = 9.332(4), c = 5.136(2) Å coinciding within uncertainty with the published data.[18]

It should be noted that the compound ***β*-Na$_2$[IrF$_6$]** is metastable and, similar to $Na_2[SnF_6]$,[32] it is converted to the tetragonal phase stable at room temperature with the progress of time. The diffraction pattern of a sample of ***β*-Na$_2$[IrF$_6$]** stored in a closed vial for two years exhibited reflections of the tetragonal phase ***α*-Na$_2$[IrF$_6$]**. The refinement of unit cell parameters gave the following data: sp. gr. $P4_2/mnm$, a = 5.005(2), c = 10.074(4) Å (Figure 2).

A comparison of ***α*-Na$_2$[IrF$_6$]** and ***β*-Na$_2$[IrF$_6$]** structures calculated by the Rietveld method using TOPAS v. 6.0[33]

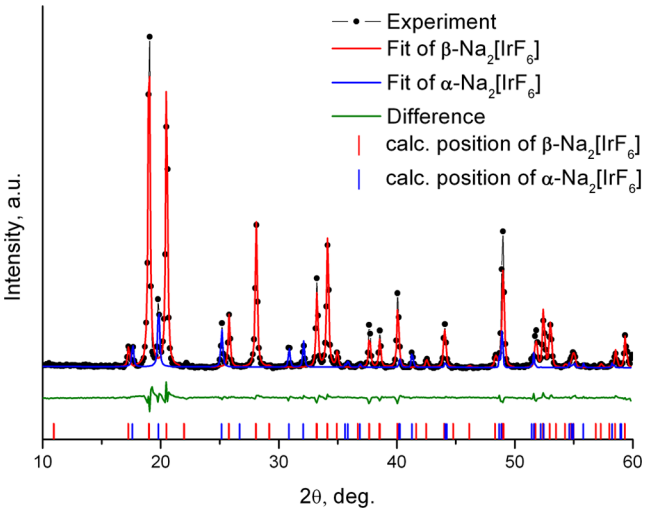

Figure 2. Powder diffraction pattern of a mixture of ***α*-Na$_2$[IrF$_6$]** and ***β*-Na$_2$[IrF$_6$] (I)** and its full-profile refinement.

software is shown in Table 1. The structure of ***α*-Na$_2$[IrF$_6$]** is slightly denser due to the stronger interaction between sodium and fluorine.

Table 1. Comparison of *α*-Na$_2$[IrF$_6$] and *β*-Na$_2$[IrF$_6$]

substance	bond distances in $[IrF_6]^{2-}$ (Å)		bond distances in $\{NaF_6\}$ (Å)		calculated density (g/cm^3)
α-Na$_2$[IrF$_6$], low temp.	Ir-F1 (4x)	1.946	Na-F1 (2x)	2.248	4.63
	Ir-F2 (2x)	1.940	Na-F1 (2x)	2.284	
			Na-F2 (2x)	2.354	
	average	1.943	average	2.295	
β-Na$_2$[IrF$_6$], high temp.	Ir1-F1 (6x)	1.940	Na1-F2 (2x)	2.204	4.52
	Ir2-F2 (3x)	1.947	Na1-F3 (2x)	2.322	
	Ir2-F2 (3x)	1.933	Na2-F1 (2x)	2.407	
	mean	1.940	mean	2.311	

The obtained single crystals of **Na$_2$[IrF$_6$]·2H$_2$O (II)** were examined by single-crystal XRD. The crystal data of **(II)** **is as follows**: $C2/m$, a = 6.6327(4) Å, b = 10.0740(6) Å, c = 5.9283(5)Å, β = 122.3880(10)° (ICSD #1955565). The powder diffraction pattern of the bulk sample of **(II)** confirmed the analytical and phase purity of the product.

The interaction of 1.009 g of ***β*-Na$_2$[IrF$_6$] (I)** with 10 ml of H^+-form of the cation exchanger KU-2 in 10 ml of water under stirring for 30 min (100 rpm) afforded a solution of **H$_2$[IrF$_6$] (III)**. After the removal of the resin by filtration, the solution volume was added to 20 ml with the addition of water and the expected concentration C(Ir) was 0.143 M. The resultant solution was titrated with aqueous NaOH to give the proton content $C(H^+)$ of 0.289 M; the iridium concentration C(Ir) of 0.120 M was also determined by UV−vis spectroscopy.[34] The determined concentration is less than the expected value, apparently, because of the partial sorption of iridium by the cation resin. Alkali titration gave only one equivalence point; hence, the solution is a strong acid in both steps. The reported behavior[25] of **(III)** as a mixture of the strong acid in the first

https://doi.org/10.1021/acsomega.1c02722
ACS Omega 2021, 6, 27697−27701

two steps and a weak acid in the third step has not been confirmed by us.

As reported in the literature,[25] preparations of the crystals of **$H_2[IrF_6]$ (III)** appeared to be unsuccessful. We expect that they can be prepared by the crystallization of IrF_4 from anhydrous HF; however, such an experiment has not been carried out for technical reasons. The solution of **(III)** was used by us for the preparation of a series of salts; however, this contribution is related to only the synthesis of sodium salts, including the preparation from the acid **(III)**.

The interaction of an aqueous solution of **$H_2[IrF_6]$ (III)** with sodium chloride, followed by a low concentration in the air, gave large yellow crystals that were identified by single-crystal XRD (by the method described below) as **$Na_3[IrF_6]\cdot 2H_2O$ (IV)** (*R*-3, a = 7.5963(3), b = 7.5963(3), c = 9.8056(4) Å) (ICSD #1955580).

$$H_2[IrF_6] + 3NaCl + 2H_2O \rightarrow Na_3[IrF_6]\cdot 2H_2O + 1/2\,Cl_2 + 2HCl$$

The powder diffraction pattern of the product **(IV)** prepared via interaction of **(III)** with a threefold excess of sodium chloride perfectly coincides with the pattern predicted from the single-crystal data (Figure 3).

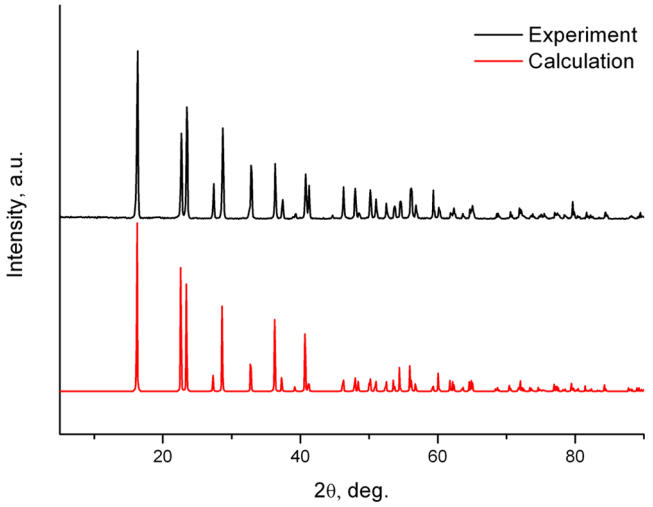

Figure 3. Powder diffraction pattern of **$Na_3[IrF_6]\cdot 2H_2O$ (IV)** and its comparison to the pattern predicted using the single-crystal data.

A gentle attempt to slowly remove water from **$Na_3[IrF_6]\cdot 2H_2O$ (IV)** by stepwise heating to 150 °C (step size of 10 °C) with thermal equilibration at 10−30 min resulted in a weight loss of ∼3% (theoretical water content 8.76%). According to the PXRD, the sample was an almost pure phase of **(IV)**, so the partial removal of water did not result in an essential structural rearrangement of **(IV)**. On heating up to 450 °C, the sample completely lost water within the temperature range of 135−400 °C, and underwent further slow partial decomposition (not more than 5%; Figure 4)

$$Na_3[IrF_6]\cdot 2H_2O \rightarrow Na_3[IrF_6]\cdot H_2O + H_2O\uparrow\ (t = 135 - 185\ ^\circ C)$$

$$Na_3[IrF_6]\cdot 2H_2O \rightarrow Na_3[IrF_6] + H_2O\uparrow\ (t = 200 - 400\ ^\circ C)$$

$$2Na_3[IrF_6] \rightarrow 6NaF + 2Ir + 3F_2\uparrow\ (t > 380\ ^\circ C)$$

$$4Na_3[IrF_6] + 6H_2O \rightarrow 12NaF + 4Ir + 12HF\uparrow + 3O_2\uparrow\ (t > 380\ ^\circ C)$$

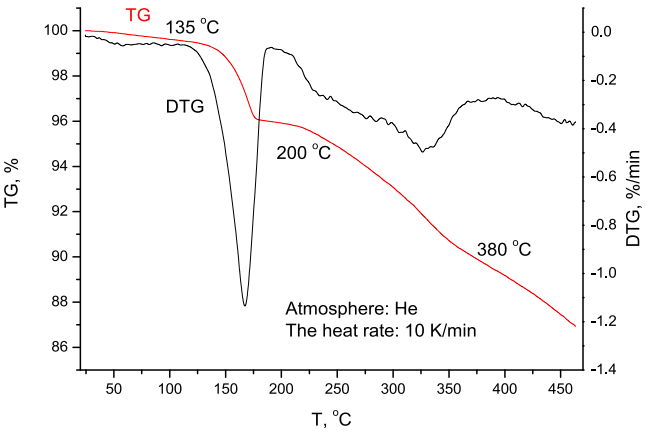

Figure 4. TGA curves of water loss and decomposition of **$Na_3[IrF_6]\cdot 2H_2O$ (IV)** in the helium atmosphere.

PXRD has demonstrated that the thermal decomposition of **$Na_3[IrF_6]\cdot 2H_2O$ (IV)** mostly afforded **$Na_3[IrF_6]$ (V)**. In addition to sodium hexafluoroiridate, the sample exhibited diffraction peaks of NaF and metallic Ir (Figure 5). The

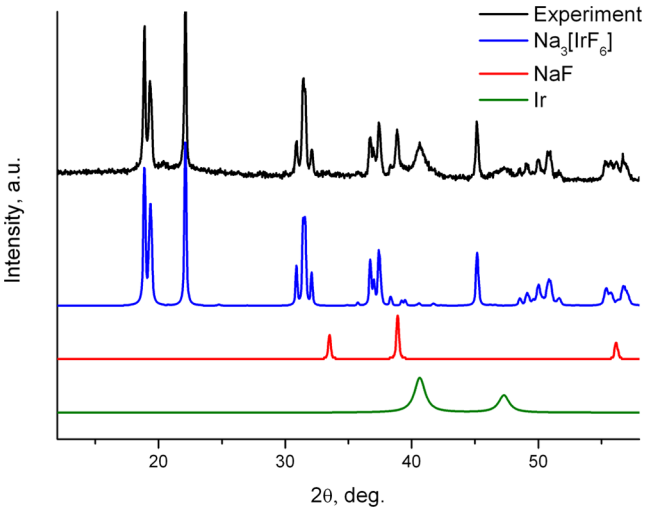

Figure 5. PXRD pattern of the products of thermal decomposition of **$Na_3[IrF_6]\cdot 2H_2O$ (IV)**. The pattern of $Na_3[IrF_6]$ was derived using the data for Ca_3TeO_6.

crystallographic data for the salt Ca_3TeO_6,[35] isostructural to previously unknown **$Na_3[IrF_6]$ (V)**, were used for full-profile fitting of the unit cell parameters of compound **(V)**: sp. gr. $P2_1/n$, a = 5.567(4), b = 5.778(4), c = 8.017(2) Å, and β = 90.41(2)°.

The common scheme of conversion in the Na(H)−Or−F(Cl) system is shown in Figure 6 ($Na_2[IrCl_6]$, $Na_2[IrCl_6]\cdot 2H_2O$, and $Na_2[IrCl_6]\cdot 6H_2O$).[36]

https://doi.org/10.1021/acsomega.1c02722
ACS Omega 2021, 6, 27697−27701

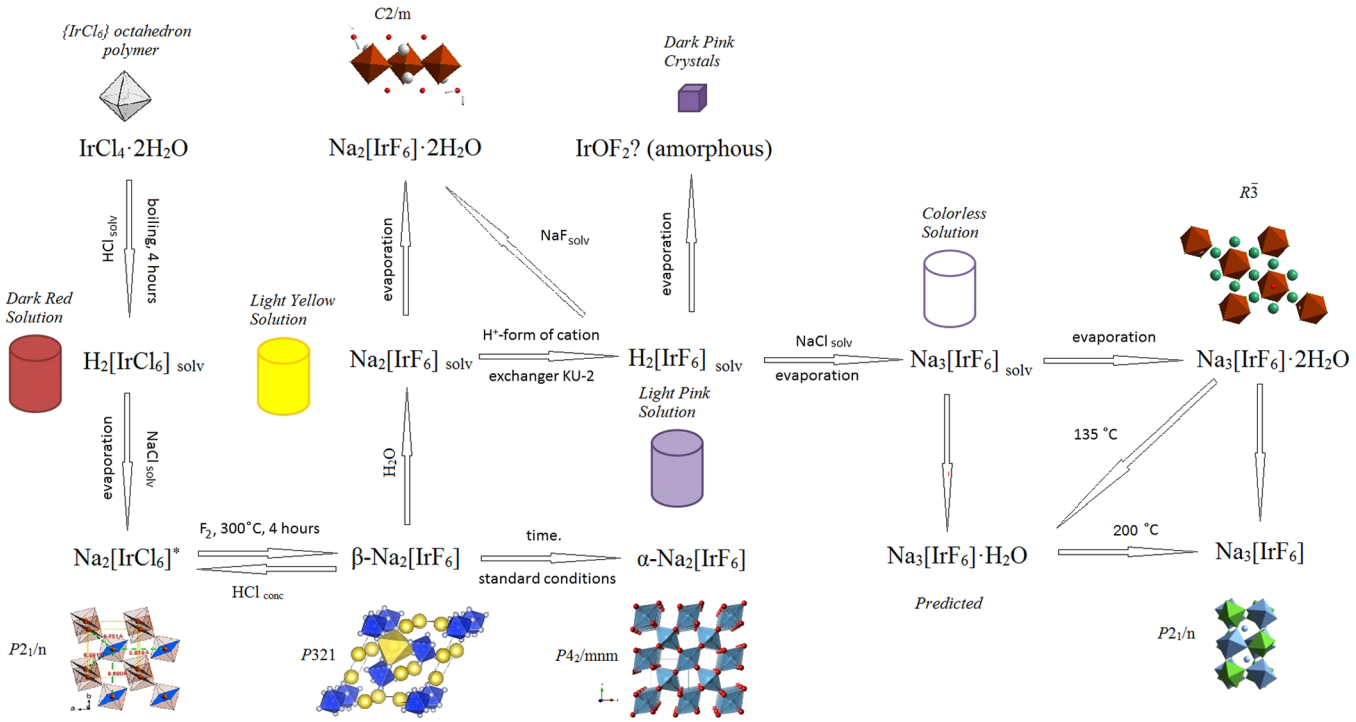

Figure 6. Common scheme of the conversion in the Na(H)−Ir−F(Cl) system.

4. CONCLUSIONS

The following salts have been synthesized and structurally characterized for the first time: $Na_2[IrF_6]\cdot 2H_2O$ ($C2/m$, a = 6.6327(4), b = 10.0740(6), c = 5.9283(5) Å, β = 122.3880(10)°) and $Na_3[IrF_6]\cdot 2H_2O$ (R-3, a = 7.5963(3), b = 7.5963(3), c = 9.8056(4) Å) by single-crystal XRD; unit cell parameters for β-$Na_2[IrF_6]$ ($P321$, a = 9.332(4), c = 5.136(2) Å) and $Na_3[IrF_6]$ ($P2_1/n$, a = 5.567(4), b = 5.778(4), c = 8.017(2) Å, β = 90.41(2)°) were determined from powder diffraction data. The crystal system and unit cell parameters of β-$Na_2[IrF_6]$ coincide within experimental uncertainty with ours and the data of Hepworth,[25] and newer results: sp. gr. $P321$, a = 9.332(4) Å, c = 5.136(2) Å. The unit cell parameters of the stable tetragonal phase α-$Na_2[IrF_6]$ ($P4_2/mnm$, a = 5.005(2), c = 10.074(4) Å) were determined for the first time. $H_2[IrF_6]$ was prepared in solution; and it was demonstrated to behave as a strong dibasic acid. The outline of the thermal decomposition curve suggests the presence of $Na_3[IrF_6]\cdot H_2O$. The common scheme of the conversion in Na(H)−Ir−F(Cl) was described.

■ ASSOCIATED CONTENT

Supporting Information

The Supporting Information is available free of charge at https://pubs.acs.org/doi/10.1021/acsomega.1c02722.

Structure of $Na_2[IrF_6]\cdot 2H_2O$ (CIF)

Structure of $Na_3[IrF_6]\cdot 2H_2O$ (CIF)

■ AUTHOR INFORMATION

Corresponding Author

Alexander I. Gubanov − *Nikolaev Institute of Inorganic Chemistry, Siberian Branch Russian Academy of Science, Novosibirsk 630090, Russian Federation;* orcid.org/0000-0002-6966-3844; Email: gubanov@niic.nsc.ru

Authors

Anton I. Smolentsev − *Nikolaev Institute of Inorganic Chemistry, Siberian Branch Russian Academy of Science, Novosibirsk 630090, Russian Federation; Novosibirsk State University, Novosibirsk 630090, Russian Federation*

Evgeny Filatov − *Nikolaev Institute of Inorganic Chemistry, Siberian Branch Russian Academy of Science, Novosibirsk 630090, Russian Federation*

Natalia V. Kuratieva − *Nikolaev Institute of Inorganic Chemistry, Siberian Branch Russian Academy of Science, Novosibirsk 630090, Russian Federation*

Andrey M. Danilenko − *Nikolaev Institute of Inorganic Chemistry, Siberian Branch Russian Academy of Science, Novosibirsk 630090, Russian Federation*

Sergey Vasilievich Korenev − *Nikolaev Institute of Inorganic Chemistry, Siberian Branch Russian Academy of Science, Novosibirsk 630090, Russian Federation*

Complete contact information is available at: https://pubs.acs.org/10.1021/acsomega.1c02722

Notes

The authors declare no competing financial interest.

■ ACKNOWLEDGMENTS

This work was supported by the Russian Science Foundation, grant number 21-73-20203 (in the part of synthesis $Na_2[IrF_6]$ and $Na_2[IrCl_6]$), and by the Ministry of Science and Higher Education of the Russian Federation, project number 121031700315-2 (in the part of chemistry investigation synthesized compounds in water and under thermal action).

■ REFERENCES

(1) Rau, J. G.; Lee, E. K.-H.; Kee, H.-Y. Spin-Orbit Physics Giving Rise to Novel Phases in Correlated Systems: Iridates and Related Materials. *Annu. Rev. Condens. Matter Phys.* **2016**, 7, 195−221.

(2) Meyers, D.; Cao, Y.; Fabbris, G.; Robinson, N. J.; Hao, L.; Frederick, C.; Traynor, N.; Yang, J.; Lin, J.; Upton, M. H.; Casa, D.; Kim, J.-W.; Gog, T.; Karapetrova, E.; Choi, Y.; Haskel, D.; Ryan, P. J.; Horak, L.; Liu, X.; Liu, J.; Dean, M. P. M. Magnetism in iridate heterostructures leveraged by structural distortions. *Sci. Rep.* **2019**, *9*, No. 4263.
(3) Kim, B. J.; Ohsumi, H.; Komesu, T.; Sakai, S.; Morita, T.; Takagi, H.; Arima, T. Phase-sensitive observation of a spin-orbital Mott state in Sr_2IrO_4. *Science* **2009**, *323*, 1329−1332.
(4) Kim, Y. K.; Krupin, O.; Denlinger, J. D.; Bostwick, A.; Rotenberg, E.; Zhao, Q.; Mitchell, J. F.; Allen, J. W.; Kim, B. J. Fermi arcs in a doped pseudospin-1/2 Heisenberg antiferromagnet. *Science* **2014**, *345*, 187−190.
(5) Kim, Y. K.; Sung, N. H.; Kim, B. J.; et al. Observation of a d-wave gap in electron-doped Sr_2IrO_4. *Nat. Phys.* **2016**, *12*, 37−41.
(6) Zhao, L.; Torchinsky, D. H.; Chu, H.; Ivanov, V.; Lifshitz, R.; Flint, R.; Qi, T.; Cao, G.; Hsieh, D. Evidence of an odd-parity hidden order in a spin-orbit coupled correlated iridate. *Nat. Phys.* **2016**, *12*, 32−37.
(7) Yang, B.-J.; Kim, Y. B. Topological insulators and metal-insulator transition in the pyrochlore iridates. *Phys. Rev. B.* **2010**, *82*, No. 085111.
(8) Wan, X.; Turner, A. M.; Vishwanath, A.; Savrasov, S. Y. Topological semimetal and Fermi-arc surface states in the electronic structure of pyrochlore iridates. *Phys. Rev. B: Condens. Matter Mater. Phys.* **2011**, *83*, No. 205101.
(9) Witczak-Krempa, W.; Kim, Y. B. Topological and magnetic phases of interacting electrons in the pyrochlore iridates. *Phys. Rev. B* **2012**, *85*, No. 045124.
(10) Donnerer, C.; Pincini, D.; Strempfer, J.; Krisch, M.; Prabhakaran, D.; Boothroyd, A. T.; McMorrow, D. F.; et al. All-in−all-Out Magnetic Order and Propagating Spin Waves in $Sm_2Ir_2O_7$. *Phys. Rev. Lett.* **2016**, *117*, No. 037201.
(11) Fujioka, J.; Yamada, R.; Kawamura, M.; Sakai, S.; Hirayama, M.; Arita, R.; Okawa, T.; Hashizume, D.; Hoshino, M.; Tokura, Y. Strong-correlation induced high-mobility electrons in Dirac semimetal of perovskite oxide. *Nat. Commun.* **2019**, *10*, No. 362.
(12) Machida, Y.; Nakatsuji, S.; Onoda, S.; Tayama, T.; Sakakibara, T. Time-reversal symmetry breaking and spontaneous Hall effect without magnetic dipole order. *Nature* **2010**, *463*, 210−213.
(13) Modic, K. A.; Smidt, T. E.; Kimchi, I.; Breznay, N. P.; Biffin, Al.; Choi, S.; Johnson, R. D.; Coldea, R.; Watkins-Curry, P.; McCandless, G. T.; Chan, J. Y.; Gandara, F.; Islam, Z.; Vishwanath, A.; Shekhter, A.; McDonald, R. D.; Analytis, J. G. Realization of a three-dimensional spin-anisotropic harmonic honeycomb iridate. *Nat. Commun.* **2014**, *5*, No. 4203.
(14) Nishimoto, S.; Katukuri, V. M.; Yushankhai, V.; Stoll, H.; Rößler, U. K.; Hozoi, L.; Rousochatzakis, I.; Van den Brink, J. Strongly frustrated triangular spin lattice emerging from triplet dimer formation in honeycomb Li_2IrO_3. *Nat. Commun.* **2016**, *7*, No. 10273.
(15) Gordon, J. S.; Catuneanu, A.; Sørensen, E. S.; Kee, H.-Y. Theory of the field-revealed Kitaev spin liquid. *Nat. Commun.* **2019**, *10*, No. 2470.
(16) Bhowal, S.; Satpathy, S. Electric field tuning of the anomalous Hall effect at oxide interfaces. *npj Comput. Mater.* **2019**, *5*, No. 61.
(17) Birol, S.; Haule, K. Jeff 1/4 1/2 Mott-insulating state in Rh and Ir fluorides. *Phys. Rev. Lett.* **2015**, *114*, No. 096403.
(18) Pedersen, K. S.; Bendix, J.; Tressaud, A.; Durand, E.; Weihe, H.; Salman, Z.; Morsing, T. J.; Woodruff, D. N.; Lan, Y.; Wernsdorfer, W.; Mathoniere, C.; Piligkos, S.; Klokishner, S. I.; Ostrovsky, S.; Ollefs, K.; Wilhelm, F.; Rogalev, A.; Clerac, R. Iridates from the molecular side. *Nat. Commun.* **2016**, *7*, No. 12195.
(19) Rossi, M.; Retegan, M.; Giacobbe, C.; Fumagalli, R.; Efimenko, A.; Kulka, T.; Wohlfeld, K.; Gubanov, A. I.; Sala, M. M. Possibility to realize spin-orbit-induced correlated physics in iridium fluorides. *Phys. Rev.* **2017**, *B 95*, No. 235161.
(20) Fitz, H.; Müller, B. G.; Graudejus, O.; Bartlett, N. Einkristalluntersuchungen an $LiMF_6$ (M = Rh, Ir), Li_2RhF_6 und K_2IrF_6. *Anorg. Allg. Chem.* **2020**, *628*, 133−137.
(21) Smolentsev, A. I.; Naumov, D. Y.; Gubanov, A. I.; Danilenko, A. M. Rubidium hexafluoridoiridate (IV). *Acta Crystallogr., Sect. E: Struct. Rep. Online* **2007**, *63*, i200.
(22) Smolentsev, A. I.; Naumov, D. Y.; Gubanov, A. I.; Danilenko, A. M. Caesium hexafluoridoiridate (IV). *Acta Crystallogr., Sect. E: Struct. Rep. Online* **2007**, *63*, i201.
(23) Smolensev, A. I.; Gubanov, A. I.; Danilenko, A. M. Three hexafloridoiridates(IV), $Ca[IrF_6]\cdot 2H_2O$, $Sr[IrF_6]\bullet 2H_2O$ and $Ba[IrF_6]$. *Acta Crystallogr., Sect. C: Cryst. Struct. Commun.* **2007**, *63*, i99−i101.
(24) Isakova, V. G.; Baidina, I. A.; Morozova, N. B.; Igumenov, I. K. g-Halogenated iridium (III) acetylacetonates. *Polyhedron* **2000**, *19*, 1097−1103.
(25) Hepworth, M. A.; Robison, P. L.; Westland, G. J. 119. Complex Fluorides of Quadrivalent Osmium and Iridium and Corresponding Free Acids. *J. Chem. Soc.* **1958**, No. 611.
(26) Kraus, W.; Nolze, G.. *PowderCell 2.4, Program for the Representation and Manipulation of Crystal Structures and Calculation of the Resulting X-ray Powder Patterns*. Federal Institute for Materials Research and Testing: Berlin, Germany, 2000.
(27) *ICDD PDF-2 Release 2014*. International Centre for Diffraction Data: Swarthmore, PA, USA, 2014.
(28) Bruker AXS Inc. *APEX (Version 1.08), SAINT (Version 7.03) and SADABS (Version 2.11)*. Bruker Advanced X-Ray Solutions: Madison, Wisconsin, USA, 2004.
(29) Sheldrick, G. M. Crystal structure refinement with SHELXL. *Acta Crystallogr., Sect. C: Struct. Chem.* **2015**, *71*, 3.
(30) Zalkin, B.; Forrester, J. D.; Templeton, D. H. The crystal structure of sodium fluorosilicate. *Acta Cryst.* **1964**, *17*, 1408−1412.
(31) Babel, D. Structural Chemistry of Octahedral Fluorocomplexes of the Transition Elements. In *Structure and Bonding*; Springer: Berlin, Heidelberg, 1967; Vol. 3, pp 1−87.
(32) Grannec, J.; Fournes, L.; Lagassie, P. X-ray and Mossbauer Evidence for a High Temperature Form of Na_2SnF_6. *Mater. Res. Bull.* **1990**, *25*, 1035−1041.
(33) Coelho, A. A.. *TOPAS-Academic V.6.0 General Profile and Structure Analysis Software for Powder Diffraction Data*. http://www.topas-academic.net/, 2016.
(34) Zolotov, Y. A.; Varshal, G. M.; Ivanov, V. M. *Analiticheskaya himiya metallov platinovoy gruppy [Analytical chemistry of Platinum metals]*; Komkniga Publ: Moscow, 2005.
(35) Hottentot, D.; Loopstra, B. O. The structure of calcium orthotellurate. *Acta Crystallogr., Sect. B: Struct. Crystallogr. Cryst. Chem.* **1981**, *B37*, 220−222.
(36) Bao, S.-S.; Wang, D.; Xuang, X.-D.; Etter, M.; Cai, Z.-S.; Wan, X.; Dinnebier, R. E.; Zheng, L.-M. Na2IrIVCl6: Spin−Orbital-Induced Semiconductor Showing Hydration-Dependent Structural and Magnetic Variations. *Inorg. Chem.* **2018**, *57*, 13252−13258.

https://doi.org/10.1021/acsomega.1c02722
ACS Omega 2021, 6, 27697−27701